Molecular Plant Pathology

MOLECULAR PLANT PATHOLOGY (2020) **21**(1), 66–82 DOI: 10.1111/mpp.12880

The effector GpRbp-1 of *Globodera pallida* targets a nuclear HECT E3 ubiquitin ligase to modulate gene expression in the host

AMALIA DIAZ-GRANADOS[1], MARK G. STERKEN[1], HEIN OVERMARS[1], ROEL ARIAANS[1], MARTIJN HOLTERMAN[1], SOMNATH S. POKHARE[2,4], YULIN YUAN[3], RIKUS POMP[1], ANNA FINKERS-TOMCZAK[1,6], JAN ROOSIEN[1], ERIK SLOOTWEG[1], ABDENASER ELASHRY[2,5], FLORIAN M.W. GRUNDLER[2], FANGMING XIAO[3], ASKA GOVERSE[1] AND GEERT SMANT[1,*]

[1]*Laboratory of Nematology, Wageningen University and Research, Wageningen, Netherlands*
[2]*Department of Molecular Phytomedicine, University of Bonn, Bonn, Germany*
[3]*Department of Plant Sciences, University of Idaho, Moscow, USA*
[4]*ICAR National Rice Research Institute, Cuttack, 753006, India*
[5]*Strube Research GmbH, Hauptstrasse 1, 38387, Söllingen, Germany*
[6]*KeyGene N.V., Wageningen, Netherlands*

SUMMARY

Plant-parasitic nematodes secrete effectors that manipulate plant cell morphology and physiology to achieve host invasion and establish permanent feeding sites. Effectors from the highly expanded SPRYSEC (SPRY domain with a signal peptide for secretion) family in potato cyst nematodes have been implicated in activation and suppression of plant immunity, but the mechanisms underlying these activities remain largely unexplored. To study the host mechanisms used by SPRYSEC effectors, we identified plant targets of GpRbp-1 from the potato cyst nematode *Globodera pallida*. Here, we show that GpRbp-1 interacts in yeast and *in planta* with a functional potato homologue of the Homology to E6-AP C-Terminus (HECT)-type ubiquitin E3 ligase UPL3, which is located in the nucleus. Potato lines lacking *StUPL3* are not available, but the *Arabidopsis* mutant *upl3-5* displaying a reduced *UPL3* expression showed a consistently small but not significant decrease in susceptibility to cyst nematodes. We observed a major impact on the root transcriptome by the lower levels of AtUPL3 in the *upl3-5* mutant, but surprisingly only in association with infections by cyst nematodes. To our knowledge, this is the first example that a HECT-type ubiquitin E3 ligase is targeted by a pathogen effector and that a member of this class of proteins specifically regulates gene expression under biotic stress conditions. Together, our data suggest that GpRbp-1 targets a specific component of the plant ubiquitination machinery to manipulate the stress response in host cells.

Keywords: Cyst nematodes, GpRbp-1, HECT E3 ligase, nematode effectors, ubiquitination, UPL3, virulence/parasitism.

*Correspondence: Email: geert.smant@wur.nl

INTRODUCTION

Plant-parasitic nematodes are biotrophic pests posing a serious threat to important food crops like potato, soybean and rice. Infestation with nematodes is estimated to reduce the worldwide crop yield by 12% (Nicol *et al.*, 2011). Cyst nematodes belonging to the genera *Globodera* and *Heterodera* are among the most destructive nematode species, despite having a relatively narrow host range (Jones *et al.*, 2009). Cyst nematodes have a sedentary lifestyle, relying exclusively on nutrients provided by living host cells for their development and survival. At the onset of parasitism, soilborne infective juveniles penetrate the roots of host plants and migrate intracellularly until they settle to establish a permanent feeding site, the syncytium. The flow of nutrients is redirected from the vascular tissue towards feeding nematodes through this host-derived feeding site. On the successful establishment of a syncytium, cyst nematodes become sedentary and depend entirely on it throughout their life cycle.

The interaction between cyst nematodes and host plants involves an arsenal of effectors that nematodes secrete into infected root tissue. Nematode effectors modulate plant immunity and promote virulence by manipulating the metabolism and physiology of the plant (Gheysen and Mitchum, 2011; Mitchum *et al.*, 2013; Quentin *et al.*, 2013). Intracellular migration as well as the initiation, establishment and maintenance of the syncytium requires dramatic physiologic and metabolic reprogramming. This reprogramming of host cells is also mediated by nematode effectors (Gheysen and Mitchum, 2011; Mitchum *et al.*, 2013; Quentin *et al.*, 2013). While a large repertoire of effectors is predicted for cyst nematodes, only a small number of effectors have been functionally characterized, often by the identification of their host targets.

Host targets of cyst nematode effectors are (predicted to be) involved at different levels of cellular regulation, including the post-translational level (Hewezi *et al*., 2016; Juvale and Baum, 2018). Ubiquitination is a mechanism for post-translational regulation in which the small protein ubiquitin is covalently attached to substrate proteins (Sadanandom *et al*., 2012). Addition of mono- and polyubiquitin can influence endocytosis, protein sorting and gene expression of the substrate among others (Zhou and Zeng, 2017). Nevertheless, the most prominent role of ubiquitination is to direct proteins for degradation by the 26S proteasome, thereby regulating protein turnover in the cell (Vierstra, 2009). The hallmark for substrate degradation by the ubiquitin-26S proteasome system (UPS) is the attachment of a chain of four or more ubiquitin subunits interlinked by a conserved lysine in position 48 of the ubiquitin peptide (Vierstra, 2009).

Ubiquitination is pivotal for plant plasticity as it allows specific perception and a rapid response to differing environmental conditions (Sadanandom *et al*., 2012; Vierstra, 2009). Ubiquitination is also recurrently found to be involved in the responses of plants to biotic stress (Delauré *et al*., 2008). The plant immune system relies on surface- and cytoplasm-localized receptors to detect attempts of pathogens at invasion and colonization of the plant tissue (Bent and Mackey, 2007). Recognition by either type of receptor results in hormone-dependent signalling events that ultimately activate defence responses to fend off pathogen attacks (Pieterse *et al*., 2012). Ubiquitination has been related to the control of immune receptors as well as hormone-dependent immune signalling in the interactions of several biotrophic pathogens, like bacteria and fungi (Craig *et al*., 2009; Delauré *et al*., 2008). Conversely, the ubiquitination machinery of plants can be hijacked or mimicked by pathogens to aid in the infection process, for instance by the Avr3a effector from *Phytophtora infestans* or by AvrPtoB from *Pseudomonas syringae* (Abramovitch *et al*., 2006; Banfield, 2015; Bos *et al*., 2010). Nevertheless, the role of ubiquitination during recognition and responses to nematode invasion remains largely unexplored (Chronis *et al*., 2013; Hewezi, 2015; Kud *et al*., 2019).

The importance of ubiquitination as a major regulator of plant responses is reflected in a large portion of plant genes encoding components of the ubiquitination and proteasome machinery. For example, 6% of the genome of *Arabidopsis thaliana* is estimated to encode proteins involved in ubiquitination (Serrano *et al*., 2018; Vierstra, 2009). Ubiquitination follows an ATP-dependent cascade mediated by three enzymes. E1 ubiquitin-activating enzymes transfer ATP to ubiquitin to activate it (Sadanandom *et al*., 2012). Subsequently, E2 ubiquitin-conjugating enzymes form a stable intermediate with activated ubiquitin, which is transferred to the final substrate by E3 ubiquitin ligases (E3 ligases) (Sadanandom *et al*., 2012). E3 ligases define the substrate specificity of the ubiquitination complex and therefore play a central role in the control of this post-translational modification (Mazzucotelli *et al*., 2006; Shu and Yang, 2017). The 26S proteasome recognizes and degrades ubiquitinated substrates to maintain tight regulation of protein turnover in the cell (Sadanandom *et al*., 2012; Vierstra, 2009). Finally, after substrate breakdown, ubiquitin subunits are recycled by deubiquitinating enzymes (Sadanandom *et al*., 2012; Vierstra, 2009). Of the enzymes involved in ubiquitination, the E3 ligases are the most abundant in plant genomes. Two E1s, approximately 35 E2s and 50 deubiquitinating enzymes are predicted to be encoded in the *Arabidopsis* genome (Miricescu *et al*., 2018). In contrast, the *Arabidopsis* genome harbours over 1500 genes encoding E3 ligases (Miricescu *et al*., 2018). Plant E3 ligases are divided into families depending on their structure and catalytic mechanism. E3 ligases containing a Homology to E6-AP C-Terminus (HECT) domain are monomeric proteins that bind directly both the E2 and the substrate. In this way, HECT E3 ligases serve as an intermediary by forming a covalent bond with ubiquitin that is later transferred to the final substrate protein (Downes *et al*., 2003).

GpRbp-1 is a prototypical effector from the potato cyst nematode *Globodera pallida*. It is produced in the dorsal oesophageal gland of the nematode (Blanchard *et al*., 2005), where part of the salivary secretions of the nematode are produced. Furthermore, it is abundantly expressed in the early parasitic stages of the nematode life cycle. Therefore, GpRbp-1 is believed to play a role during the initiation and/or establishment of syncytia (Blanchard *et al*., 2005). Additionally, specific variants of GpRbp-1 are recognized by the potato immune receptor Gpa2, leading to cell death on co-expression by agroinfiltration in *Nicotiana benthamiana* leaves (Sacco *et al*., 2009). Interestingly, GpRbp-1 variants remain under positive selection, indicating that at least some members of this effector family play an important role in the virulence of *G. pallida* (Carpentier *et al*., 2012). GpRbp-1 belongs to the highly expanded SPRYSEC (SPRY domain with a signal peptide for secretion) family of effectors in potato cyst nematodes, characterized by an N-terminal signal peptide for secretion and a C-terminal SPRY (splA, spore lysis A and RyR, ryanodine receptor) domain (Ali *et al*., 2015; Diaz-Granados *et al*., 2016; Rehman *et al*., 2009). The N-terminal signal peptide indicates that GpRbp-1 is likely delivered by the nematode to the plant cell, where it can interact with plant targets. This may involve the C-terminal SPRY domain, which is believed to function as a protein-binding platform required for the virulence role of SPRYSEC effectors, as shown for effector SPRY-414-2 from *G. pallida* (Mei *et al*., 2018).

To elucidate the host mechanisms used by GpRbp-1 in the virulence of *G. pallida*, we aimed to characterize its molecular targets in host plant cells. Here, we show that the nematode effector GpRbp-1 interacts specifically in yeast and *in planta* with a potato E3 ubiquitin protein ligase (StUPL3). Moreover, we demonstrate by bimolecular fluorescence complementation (BiFC) that this interaction most likely occurs in the nucleus. These data suggest that this HECT E3 ligase may be required for infection by *G. pallida*. Due to the lack of a StUPL3 knock-out mutant in potato,

we examined the role of *A. thaliana* AtUPL3 in nematode virulence using the beet cyst nematode *Heterodera schachtii,* which exploits the same mode of parasitism as *G. pallida*. We found that inoculation of the *Arabidopsis* knock-down mutant *upl3-5* revealed a consistently small, but statistically not significant, reduction of susceptibility to *H. schachtii* as compared to the wild-type plants, suggesting that UPL3 may only have a minor contribution to cyst nematode parasitism. However, a strong transcriptional regulation in *Arabidopsis* plants was only observed by microarray analysis of nematode-infected *upl3-5* roots. Interestingly, this transcriptional regulation involves genes that are related to stress responses, suggesting that cyst nematodes modulate host gene expression in plant cells through targeting of UPL3 in the nucleus. To the best of our knowledge, this is the first report of a plant-parasitic nematode effector targeting the host ubiquitination machinery by interacting with a plant HECT E3 ligase.

RESULTS

GpRbp-1 interacts with a fragment of ubiquitin E3 ligase UPL3 from potato

To find plant interactors of GpRbp-1, we performed a yeast two-hybrid screen of a cDNA library of 3.85×10^6 clones obtained from susceptible potato roots infected with *G. pallida*. Using GpRbp-1 from *G. pallida* virulent population Rookmaker as bait, we found two yeast clones harbouring an identical insert sequence of 413 bp that showed the highest similarity to *A. thaliana* E3 ubiquitin protein ligase UPL3 (GenBank accession XP_006359694.1; e-value 2.11287×10^{-42} in BLASTX on the non-redundant database at NCBI). Therefore, we named the interacting fragment StUPL3frag8. In *Arabidopsis*, UPL3 is composed of an N-terminal Armadillo repeat domain (Pfam16186) and a C-terminal catalytic HECT domain (Pfam00632) (Marchler-Bauer and Bryant, 2004; Marchler-Bauer *et al.*, 2017). StUPL3frag8 localizes to the C-terminal half of UPL3, in the HECT domain of the protein (Fig. 1A,B, Fig. S1).

To investigate the similarity of UPL3 from *A. thaliana* and potato, we compared the coding and peptide sequence of both genes using a CLUSTALW alignment. We obtained the full-length coding sequence for StUPL3 from the non-redundant nucleotide database of GenBank (XM_015314510). At the nucleotide level, AtUPL3 and StUPL3 are 67% identical (data not shown) and at the protein level they share 70% identity (Fig. S1). It should be noted that StUPL3frag8 was 98% identical to StUPL3 from NCBI (Fig. 1B, Fig. S1). Furthermore, we investigated the number of copies of *StUPL3* present in the genome sequence of the doubled monoploid potato genotype DM. To this end, we queried with a BLASTN algorithm the PGSC *Solanum tuberosum* group Phureja DM1-3 transcripts v. 3.4 database from the Potato Genomics resource of Michigan University (Hirsch *et al.*, 2014) using AtUPL3 as input. We found two transcripts that match the AtUPL3 coding sequence, transcript PGSC0003DMT400031189 (1189) and transcript PGSC0003DMT400031190 (1190) (e-values 1×10^{-59} and 7×10^{-52}, respectively). Further examination of each transcript indicated that the corresponding genomic sequence is the same for both transcripts (PGSC0003DMG402011946; 11946), indicating that transcripts 1189 and 1190 are segments of the same StUPL3 coding sequence (Fig. S1A). Most likely, they remain separated in the automatic annotation as individual transcripts due to the presence of a large intron in the genomic sequence. Finally, we analysed the genomic position of the coding sequence 11946 with the SpudDB Genome Browser tool (Hirsch *et al.*, 2014). The genomic region containing sequence 11946 is located in chromosome 10 of the DM potato genotype. These results suggest that StUPL3 is encoded by a single gene that resides on chromosome 10 of the DM potato genotype.

Furthermore, to investigate if StUPL3 affects overall E3 ligase activity *in planta*, we determined whether StUPL3 can promote *in vivo* ubiquitination when expressed in plant cells. To this end, N-terminal haemagglutinin (HA)- or green fluorescence protein (GFP)-tagged StUPL3 (HA-StUPL3 or GFP-StUPL3) was co-expressed with HA-tagged ubiquitin (HA-Ub) in *N. benthamiana* leaves. Total ubiquitination with exogenous HA-Ub was expected as a smear banding pattern in a western blot using anti-HA antibodies. Indeed, exogenous HA-Ub can be used *in planta* for polyubiquitination (Fig. S1B). On expression of StUPL3 the polyubiquitination signal was increased, suggesting that StUPL3 has E3 ubiquitin ligase activity *in planta* (Fig. S1B).

To verify the specificity of the interaction of GpRbp-1 and StUPL3frag8 in yeast by swapping the yeast expression vectors, we co-transformed StUPL3frag08 in the bait configuration and GpRpb-1 as the prey into yeast strain PJ69-4a. Likewise, the nematode effector GrSPRYSEC-19 and its cognate plant interactor Sw5F were used as positive control (Rehman *et al.*, 2009), while StUPL3frag8 was co-transformed with human Lamin C into yeast as negative control. The yeast cells were grown on triple drop-out (–LWH; TDO) medium for 6 days after co-transformation, after which individual colonies were replated onto fresh TDO medium. We obtained several colonies of the co-transformation of StUPL3frag8 with GpRbp-1 and GrSPRYSEC-19 with SwF5, but none with the negative control (Fig. 1C). Therefore, we concluded that GpRbp-1 and a C-terminal fragment of E3 ligase UPL3 from potato specifically interact in yeast.

To independently confirm the interaction *in planta*, we performed co-immunoprecipitation (co-IP) assays with HA-tagged StUPL3frag8 (HA-StUPL3frag8) using Myc-GFP-tagged GpRbp-1 as bait (Myc4-GFP-GpRbp-1) on co-expression of constructs in leaves of *N. benthamiana*. HA-StUPL3frag8 alone, and also together with a Myc4-GFP vector (Myc4-GFP-EV) acted as negative controls. HA-StUPL3frag8 was only co-immunoprecipitated by Myc4-GFP-GpRbp-1 (Fig. 1D). We therefore concluded that

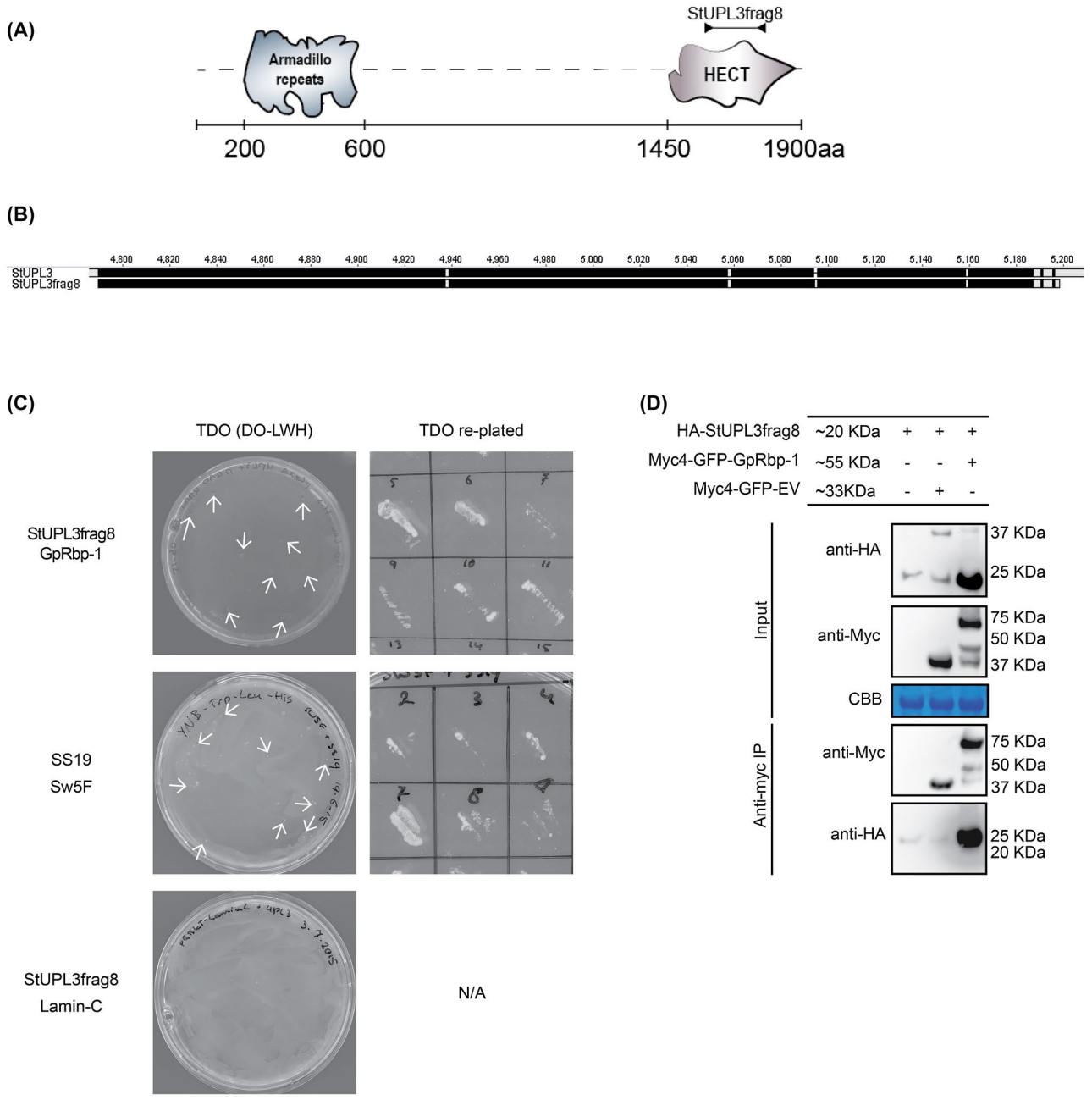

Fig. 1 GpRpb-1 interacts in yeast and *in planta* with a fragment of the E3 ubiquitin ligase UPL3 from potato. (A) Predicted domain architecture of the E3 ligase UPL3 from *Solanum tuberosum* (StUPL3). The location of the interacting StUPL3frag8 is indicated with an arrow. (B) Alignment of the coding sequences of the StUPL3DS8 fragment and full-length StUPL3 (Fig. S1). Identical residues are depicted in black and non-identical residues are shown in grey. The overall sequence identity is 97%. (C) Directed yeast two-hybrid interaction of StUPL3frag8 and GpRbp-1 in a reversed bait-prey configuration. The interaction between Sw5F and SS-19 is used as positive control (Rehman *et al.*, 2009) and human Lamin C is used as negative control. Yeast was grown on triple drop-out (TDO) medium after transformation. Colonies were only visible in the positive control and StUPL3frag8/GpRbp-1 interaction plates (arrows). Colonies grown on the TDO selection were replated to fresh TDO medium to confirm positive clones (TDO re-plated). Pictures are taken at 6 and 5 days post-transformation, respectively. (D) Co-immunoprecipitation of StUPL3frag08 (HA-StUPL3frag8) and GpRbp-1 (Myc4-GFP-GpRbp-1) or empty vector control (Myc4-GFP-EV). Proteins were extracted from *Nicotiana benthamiana* leaves 3 days after agroinfiltration.

the C-terminal fragment of UPL3 from potato obtained in the yeast screen is also able to interact specifically with GpRbp-1 *in planta.*

Remarkably, co-expression of StUPL3frag8 with Myc4-GFP-GpRbp1 resulted in differential behaviour of the peptide encoded by the UPL3 fragment on western blot. When StUPL3frag8 was

co-expressed with Myc4-GFP-GpRbp-1, it appeared consistently as a more intense band on western blots than when it was expressed with either Myc4-GFP or alone. These observations suggest that the presence of GpRbp-1 alters the expression level or protein stability of the HA-tagged StUPL3 fragment (Fig. 1D). Furthermore, it should be noted that when StUPL3frag8 was co-expressed with the Myc4-GFP-EV an oligomer of approximately twice the molecular weight of the StUPL3fragm8 also appeared on western blots.

GpRbp-1 interacts with full-length StUPL3 *in planta*

Next, we investigated if GpRbp-1 also interacts *in planta* with full-length StUPL3. We obtained the full-length coding sequence for StUPL3 by gene synthesis based on the predicted potato transcript variant X2 (GenBank accession XM_015314510, 6128bp). We first attempted to co-immunoprecipitate HA-StUPL3 in a pull-down assay with Myc4-GFP-GpRbp-1. However, the high molecular weight StUPL3 protein (*c.*210 kDa) was only consistently observed on western blots after using destructive protein extraction methods incompatible with co-IP. We therefore used bimolecular fluorescence complementation (BiFC) following transient expression in *N. benthamiana* to test the interaction of StUPL3 and GpRbp-1 *in planta*. To this end, the N-terminal half of the fluorescent protein SCFP3A was fused to GpRbp-1 (pN::GpRbp-1) and the C-terminal half of SCFP3A was fused to StUPL3 (pC::StUPL3). As negative control, we co-expressed pN::GpRbp-1 with SCFP3A fused to the viral protein NSs (pC::NSs) and pC::UPL3 with SCFP3A fused to β-glucuronidase (pN::GUS). The characteristic fluorescence of SCFP3A was only reconstituted after co-infiltration of pN::GpRbp-1 and pC::UPL3, indicating that the interaction between GpRbp-1 and StUPL3 brought the N and C halves of cyan fluorescent protein (CFP) into close proximity (Figs 2 and S2). Based on this finding, we concluded that StUPL3 is most likely a target of GpRbp-1 in host plants. As the signal of reconstituted SCFP3A was only visible in the nucleus of transformed cells, it seemed that the interaction of GpRbp-1 with StUPL3 takes place in this subcellular compartment. Furthermore, the fluorescent signal indicates that the interaction is not evenly distributed throughout the nuclei. We observed a consistent granular pattern of fluorescence throughout the nucleus in addition to discrete globules or speckles with stronger fluorescence than the rest of the nucleus. This fluorescent pattern suggests that the interaction of GpRbp-1 and StUPL3 may be associated with specific structures within the nucleus of the cell.

GpRbp-1 and StUPL3 co-localize in the nucleus of *N. benthamiana* cells

Next we determined the native subcellular localization of StUPL3 *in planta*. First, the localization of StUPL3 was predicted *in silico*, using Plant-mPLoc (Chou and Shen, 2007, 2008, 2010; Shen and Chou, 2006) and PredictProtein (Yachdav *et al.*, 2014). Both algorithms predicted StUPL3 to be located in the nucleus. Additionally, cNLS mapper (Kosugi *et al.*, 2008, 2009a, b) predicted a monopartite nuclear localization signal (NLS) composed of RAAKRARVT at position 26 of the amino acid sequence, with score 7, suggesting a partial localization to the nucleus. The same amino acid sequence was identified by LOCALIZER (Sperschneider *et al.*, 2017) as an NLS, together with KKEPPQEKNGSSSKGKGK starting at position 1024 (Fig. S1A).

We used confocal laser scanning microscopy to evaluate the subcellular localization of N-terminally mCherry (mCh)-tagged GpRbp-1 (mCh-GpRbp-1) and N-terminally GFP-tagged StUPL3 (GFP-UPL3) when agroinfiltrated in *N. benthamiana* cells (Figs 3 and S3). mCh-GpRbp-1 and GFP-UPL3 were infiltrated together or in combination with the corresponding GFP or mCh vectors as negative controls. Individually, GpRbp-1 displayed the same nucleocytoplasmic partitioning that has been reported before (Jones *et al.*, 2009), whereas GFP-StUPL3 alone showed a specific localization in the nucleus of individually transformed cells. Moreover, on co-expression of mCh-GpRbp-1 and GFP-UPL3, the subcellular localization of both proteins remained largely unchanged. We therefore concluded that co-expression did not result in the translocation of either GpRbp-1 or StUPL3, and that they co-localize exclusively in the nucleus, consistent with the results obtained in the BiFC assay. Interestingly, the pattern of GFP-StUPL3 localization resembled the granular distribution observed for the interaction of GpRbp-1 and StUPL3 using BiFC. The fluorescent signal of GFP-StUPL3 was granular throughout the nucleus and was stronger in discrete speckles. Additionally, the granular fluorescence observed for GFP-StUPL3 was not altered by co-expression with mCh-Rbp-1.

UPL3 is involved in cyst nematode infection of *Arabidopsis*

As stable knock-out or knock-down mutants of *StUPL3* in potato were not available, we further investigated the role of UPL3 during cyst nematode infections in *A. thaliana*. In addition, beet cyst nematode *H. schachtii* is the most-related cyst nematode species to *G. pallida* capable of infecting *Arabidopsis*. To evaluate the importance of AtUPL3 for the susceptibility of *Arabidopsis* to *H. schachtii,* we counted the number of nematodes in roots of wild-type *A. thaliana* Col-0 and homozygous *upl3-5* knock-down mutant plants 2 weeks after inoculation (Fig. 4B). The *upl3-5* mutant carried a homozygous T-DNA insertion that does not result in an obvious morphological plant growth phenotype (data not shown). However, we found fewer nematodes in *upl3-5* mutant plants compared to wild-type plants (7% fewer nematodes; ANOVA, combining replications with a fixed-effect model $P = 0.150$; Fig. 4B). The T-DNA insert in *upl3-5* does not result in a full knock-out of UPL3 (Table S1), which may lead to an underestimation of the effect of

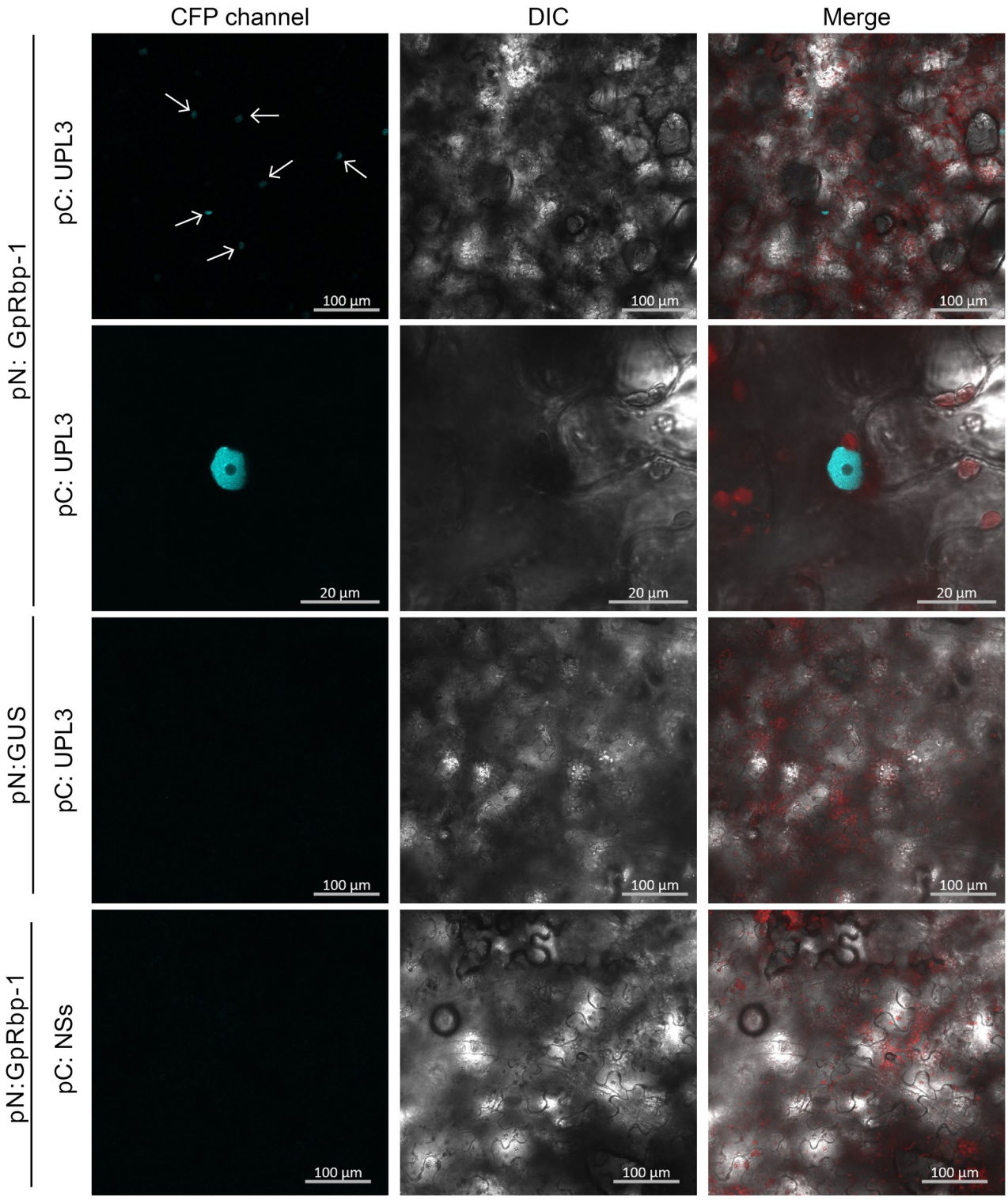

Fig. 2 GpRpb1 interacts with full-length StUPL3 in the plant nucleus. Bimolecular fluorescence complementation of subfragments of cyan fluorescent protein SCFP3a by co-expression of SCFP3A amino acids 1–173 fused to GbRpb-1 (pN::GpRbp-1) and SCFP3A amino acids 156–239 fused to StUPL3 (pC::UPL3). Co-expression of pN::GUS or pC::NSs was used as negative control. The fusion constructs were agroinfiltrated in leaves of *Nicotiana benthamiana*. Images of live cells were taken at 2 days post-infiltration and fluorescence was monitored with confocal laser scanning microscopy. Cyan fluorescent protein (CFP) emission is shown in blue, light emission in white in the differential interference contrast (DIC) channel and chloroplast autofluorescence is shown in red in the merge panel. Arrows indicate nuclei with fluorescent signal. Representative images from two leaves, from two individual plants, in three independent experiments.

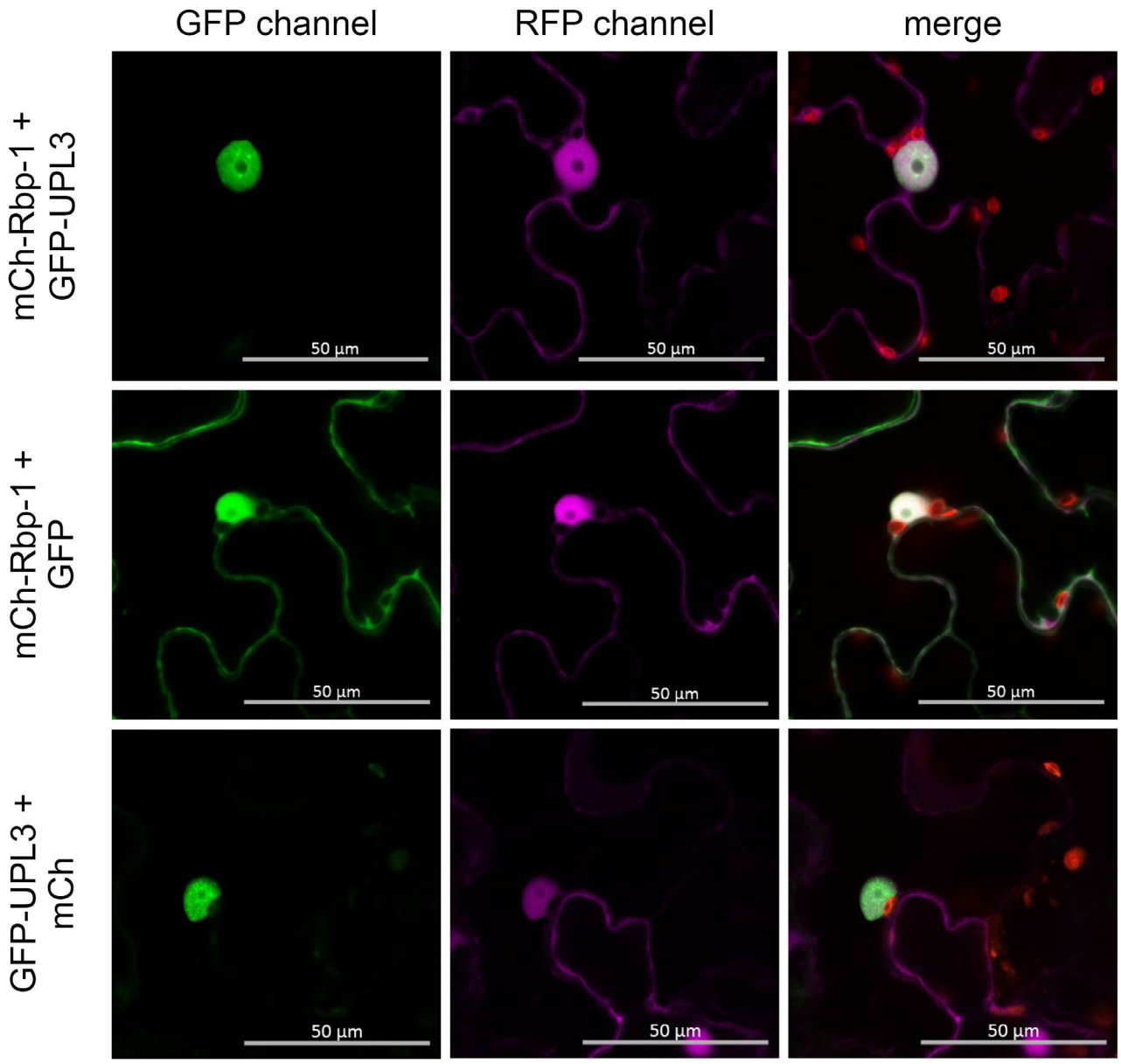

Fig. 3 GpRbp-1 and full-length StUPL3 co-localize to the nucleus of *Nicotiana benthamiana* cells. Live imaging of *N. benthamiana* leaves agroinfiltrated with combinations of protein fusions of green fluorescent protein with StUPL3 (GFP-UPL3), red fluorescent protein mCherry (mCh-GpRbp-1) or GFP and mCh alone. The emission channel for GFP is shown in green and the RFP channel for mCherry in purple. Imaging was done at 2 days post-infiltration. Representative images from two leaves, from two individual plants, in three independent experiments.

the gene during nematode infection in this mutant. We therefore also analysed the size of the syncytia established by the nematodes and the size of distinguishable females 14 days after inoculation as a parameter for successful establishment of a parasitic relationship with their host. The females and the syncytia formed in the roots of the *upl3-5* mutant seemed slightly smaller compared to wild-type plants (7% and 5%, respectively; ANOVA, combining replications with a fixed-effect model, $P = 0.075$ and $P = 0.466$, respectively; Fig. 4C). Additionally, we investigated if AtUPL3 was regulated at the transcript level in nematode-infected roots. To measure the expression of *AtUPL3*, we performed reverse transcriptase polymerase chain reaction (RT)-PCR in *A. thaliana* roots infected with *H. schachtii* or mock infected 2, 7, 10 and 14 days after inoculation. We did not find a significant infection-dependent regulation of *AtUPL3* as compared to reference genes *UBP22* and *UBQ5* (Fig. S4) (Anwer *et al.*, 2018; Hofmann and Grundler, 2007).

As we suspected that the manipulation of UPL3 by cyst nematodes could have a subtler effect on virulence than the

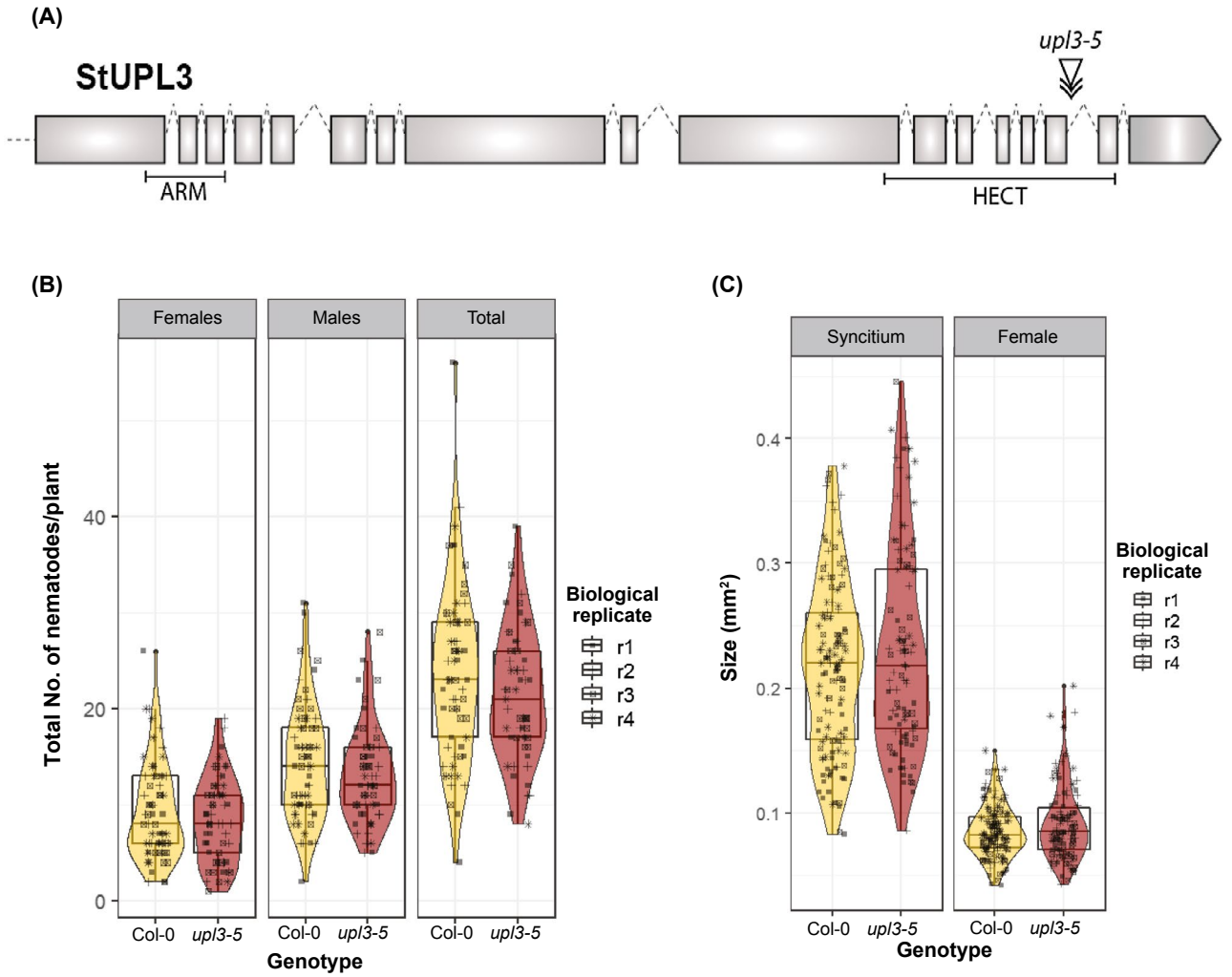

Fig. 4 Knock-down of UPL3 in *upl3-5* only slightly reduces susceptibility of *Arabidopsis* to the beet cyst nematode *Heterodera schachtii*. (A) Position of the T-DNA insert in *AtUPL3* in *Arabidopsis upl3-5* (arrowed). (B) Total number of nematodes per plant. (C) Average surface area (mm^2) of female nematodes and syncytia present in the roots of *upl3-5 Arabidopsis* line and wild-type (Col-0), after 2 weeks of infection. Whiskers indicate the quartile (25 or 75%) ± 1.5× interquartile range. Results are combined measurements from four independent biological repeats, using a fixed effects model. For (B) $n_{Col\text{-}0} = 63$ and $n_{upl3\text{-}5} = 59$. For (C) $n_{Col\text{-}0} = 127$ and $n_{upl3\text{-}5} = 106$ for syncytia, and $n_{Col\text{-}0} = 129$ and $n_{upl3\text{-}5} = 108$ for females. Statistical significance of the differences in the amount or size of nematodes infecting the roots of *upl3-5* lines and the wild-type control were established by one-way ANOVA ($\alpha = 0.05$).

detection power of our bioassays, we performed a whole transcriptome analysis in roots of the *upl3-5* mutant line and wild-type *Arabidopsis* plants inoculated with *H. schachtii*. To this end, we collected whole roots of *A. thaliana* plants at time of inoculation (0 days post-inoculation, dpi) and at 7 dpi with infective juveniles of *H. schachtii* or mock inoculation in four replicates per genotype per treatment. The impact of these conditions on the transcriptome of *Arabidopsis* was first analysed with principal component analysis. The first two principal components (PCOs) captured 68.0% of the variation and separated the effect of plant development during the 7 days after the time of inoculation (PCO 1) and the effect of nematode infection (PCO 2) (Fig. S5). Next, we tested the number of differentially expressed genes within each condition. Remarkably, the transcriptome in roots of the *upl3-5* mutant and wild-type *Arabidopsis* plants differed significantly only in the presence of *H. schachtii*. In total, 895 genes were differentially expressed between nematode-infected roots of the *upl3-5* mutant and wild-type *Arabidopsis* plants at 7 dpi [linear model, $P < 0.0001$; false discovery rate (FDR) = 0.0041] (Fig. 5C and Table S1). In contrast, only 72 genes were differentially regulated between *upl3-5* and wild-type plants at 0 dpi (linear model, $P < 0.0001$; FDR = 0.051), while 53 genes were differentially expressed between mock-infected *upl3-5* and wild-type plants at 7 dpi (linear model, $P < 0.0001$; FDR = 0.064). These results show that despite the lack of a strong effect on nematode development

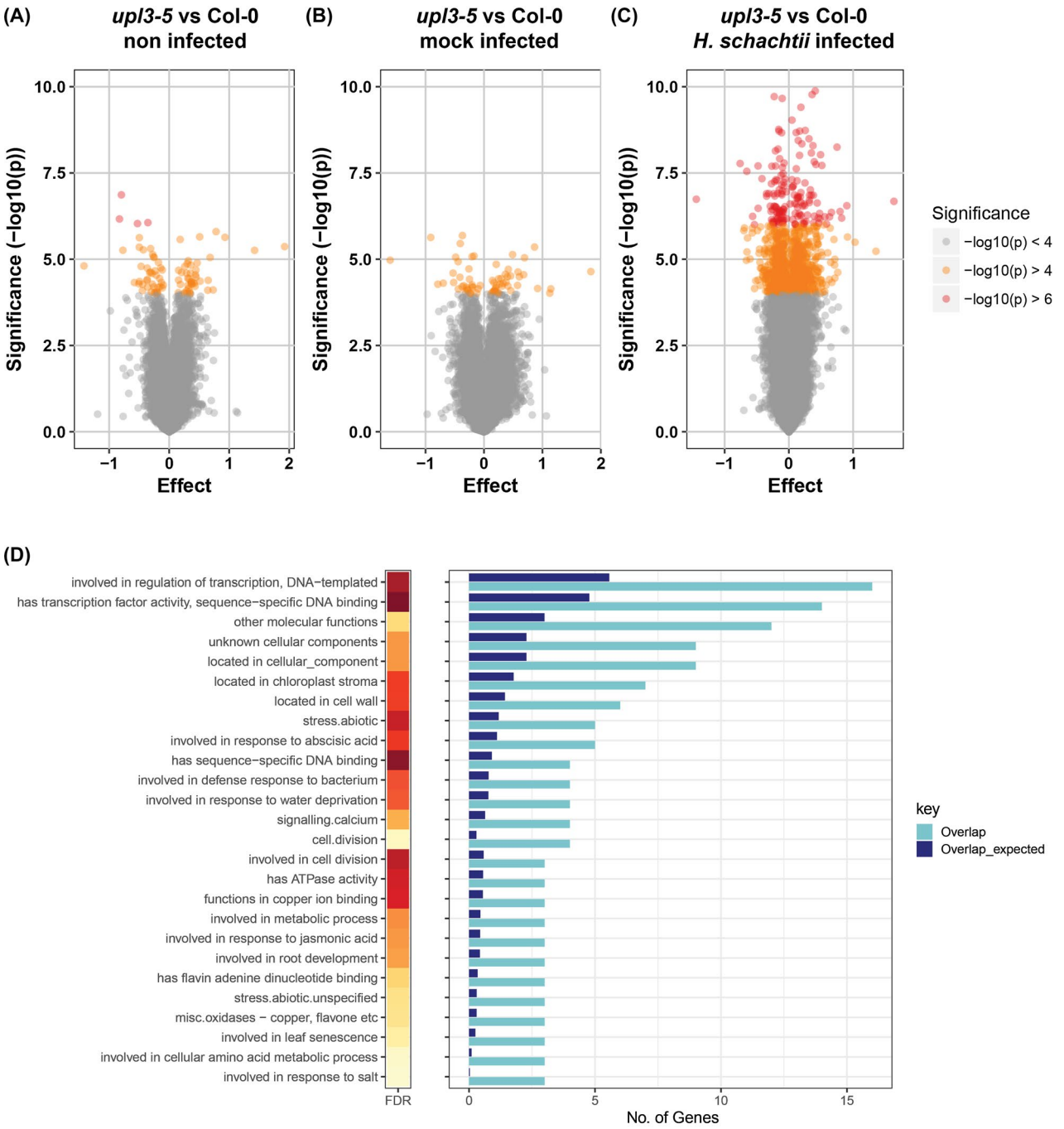

Fig. 5 AtUPL3 strongly regulates gene expression in nematode-infected roots of *Arabidopsis*. (A)–(C) Volcano plots of differential gene expression as determined by microarray analysis. (A) Genes differentially regulated in roots of *upl3-5* and wild-type *Arabidopsis* prior to nematode inoculation. The *x*-axis shows the relative expression of genes. The *y*-axis shows the significance of the differences in expression levels. Colours provide a visual aid for the thresholds in the legend. (B) Genes differentially regulated in mock-infected roots of *upl3-5* and wild-type *Arabidopsis* plants 7 days after inoculation. (C) Genes differentially regulated in roots of *upl3-5* and wild-type *Arabidopsis* plants infected with *Heterodera schachtii* 7 days after inoculation. (D) Gene ontology term enrichment analysis (hypergeometric test, false discovery rate, FDR, correction, $q < 0.05$) of the annotations of the 131 differentially regulated genes in (C). Overlap_expected indicates the number of genes that would be assigned to each category in a random sampling. Overlap shows the number of genes differentially regulated in our dataset.

Table 1 Genes most differentially regulated in *upl3-5 Arabidopsis* infected with *Heterodera schachtii*

Gene	Effect	FDR	Annotation (ThaleMine)	Gene symbol
Down-regulated in upl3-5				
AT3G05950	−1.44129	1.12E−04	RmlC-like cupins superfamily protein	
AT1G29100	−0.75923	2.93E−05	Heavy metal transport/detoxification superfamily protein	
AT1G19250	−0.65480	3.77E−05	Flavin-dependent monooxygenase 1	FMO1
AT2G21900	−0.56401	2.19E−04	WRKY DNA-binding protein 59	WRKY59
AT4G27850	−0.53659	2.91E−04	Glycine-rich protein family	
AT5G60610	−0.48008	2.94E−05	F-box/RNI-like superfamily protein	
AT4G39740	−0.47864	1.61E−04	Thioredoxin superfamily protein	HCC2
AT3G27070	−0.41832	5.61E−05	Translocase outer membrane 20-1	TOM20-1
AT3G16650	−0.34724	9.37E−05	Transducin/WD40 repeat-like superfamily protein	
AT3G09940	−0.34616	9.86E−05	Monodehydroascorbate reductase	MDHAR
Up-regulated in upl3-5				
AT4G07820	1.63498	1.25E−04	CAP (cysteine-rich secretory proteins, antigen 5 and pathogenesis-related 1 protein) superfamily protein	
AT3G28345	0.79684	1.84E−04	ABC transporter family protein	ABCB15
AT4G16000	0.74938	1.50E−05	Hypothetical protein	
AT4G16008	0.66270	1.86E−04	Hypothetical protein	
AT5G05060	0.56052	2.19E−04	Cystatin/monellin superfamily protein	
AT3G21352	0.51405	2.94E−05	Transmembrane protein	
AT4G11211	0.49339	2.01E−05	Hypothetical protein	
AT3G30210	0.48315	2.33E−04	myb domain protein 121	MYB121
AT3G32030	0.47845	1.90E−04	Terpenoid cyclases/protein prenyltransferases superfamily protein	
AT4G23670	0.46457	2.75E−04	Polyketide cyclase/dehydrase and lipid transport superfamily protein	

Top 10 most up- or down-regulated genes in the *upl3-5* mutant categorized by the size of the effect as determined by a linear model. The annotation and gene symbols or names were obtained from the ThaleMine database of Araport (Krishnakumar *et al.*, 2015). FDR, false discovery rate.

and syncytium formation, UPL3 regulates plant gene expression in response to root infection by cyst nematodes.

Genes differentially expressed in association with *upl3-5* are linked to stress responses and metabolism

To identify the biological processes that were most likely influenced by the mutation in *AtUPL3* in association with infection by cyst nematodes, we focused on genes that showed highly significant differential expression between the *upl3-5* mutant and wild-type *Arabidopsis* plants ($-\log_{10}(P) > 6$). At 7 dpi, the expression of 131 genes was significantly affected by the mutation in *AtUPL3* (FDR < 2.9E−04). Enrichment analysis of these 131 genes based on annotation terms showed a significant over-representation of 26 categories (Fig. 5D and Table S2). The categories 'Involved in response to salt' (GO:1902074, q = 8.71392E−05) and 'Involved in cellular amino acid metabolic process' (GO:0006520, q = 7.27486E−04) were enriched with the highest statistical significance. The categories 'Involved in regulation of transcription, DNA-templated' (GO:0006355) and 'Has transcription factor activity, sequence-specific DNA binding' (GO:0003700) contained the highest number of differentially regulated genes. For example, the top 10 most significantly up-/down-regulated genes include two transcription factors (MYB121 and WRKY59; Table 1). Finally, from the top 10 most significantly up-/down-regulated genes the expression of two particular genes appeared to be exceptionally affected in nematode-infected roots of the *upl3-5* mutant line. AT4G07820 was by far the most up-regulated gene in the *upl3-5* mutant line (effect size = $2^{1.635}$), with an effect size twice as large as the second most up-regulated gene, AT3G28345 (effect size = $2^{0.797}$). In contrast, AT3G05950 was the most down-regulated gene in the *upl3-5* mutant (effect size = $2^{-1.442}$) by also approximately twice as much as the second most down-regulated gene (effect = $2^{-0.759}$). The functions of both genes are not known, but based on sequence similarity, AT4G07820 and AT3G28345 are thought to be members of the cysteine-rich secretory proteins, antigen 5 and pathogenesis-related 1 protein (CAP) superfamily and

of the RmlC-like cupins superfamily, respectively. It is worth noting that AT4G07820 and AT3G05950 have a highly specific, but common, developmental expression pattern limited to roots of *Arabidopsis* (Klepikova *et al.*, 2016). Furthermore, co-expression analysis showed a similar pattern of up- or down-regulation in most of the experimental conditions currently included in the ePlant database (Fig. S6) (Waese *et al.*, 2017). This suggests that these two genes may be involved in a gene network co-regulated with UPL3.

DISCUSSION

The effector GpRbp-1 is expressed during the onset of parasitism by the potato cyst nematode *G. pallida* and to characterize its role in the virulence of potato cyst nematodes we aimed to identify the host target(s) of GpRbp-1. Here we show that GpRbp-1 physically interacts in yeast and *in planta* with UPL3, a functional HECT-type E3 ligase from a potato genotype lacking major resistances to *G. pallida*. Additionally, we demonstrated that ectopic StUPL3 and GpRbp-1 co-localize in the nucleus of *N. benthamiana* plants, where they also interact. Our data show for the first time a specific and robust interaction of a pathogen effector with a plant HECT ubiquitin E3 ligase. Together, these results suggest that StUPL3 is a host target of *G. pallida* in nematode parasitism.

Ubiquitination is a post-translational modification that is well established as a key regulator of plant responses during plant–parasite interactions (Banfield, 2015). However, the involvement or recruitment of the ubiquitination machinery during plant–nematode interactions is poorly understood. An example of a nematode effector that may recruit the UPS is effector GrUBCEP12 of *G. rostochiensis* (Chronis *et al.*, 2013). CEP12, a carboxyl extension protein processed from GrUBCEP12, supresses immunity mediated by intracellular immune receptors (Chronis *et al.*, 2013). In addition, effector RHAB1 from *G. pallida* was recently reported to function as a RING-type E3 ligase *in planta* and to promote susceptibility to the nematode (Kud *et al.*, 2019). The recruitment of different components of the ubiquitination machinery by nematodes might suggest that potato cyst nematodes employ a multilayered strategy to exploit the UPS system of the host. HECT-type E3 ubiquitin ligases have a distinct mechanism of action (Downes *et al.*, 2003), and UPL3 was previously found to co-immunoprecipitate with the HopM1 effector from *P. syringae* pv. *tomato* (Ustun *et al.*, 2016). Our results may therefore point towards a previously undescribed strategy to manipulate plant cells by nematodes and other plant pathogens. Recently, UPL3 has been shown to function as a proteasome-associated amplifier of immune responses activated by salicylic acid (SA) (Furniss *et al.*, 2018). Interaction of GpRbp-1 with StUPL3 may therefore interfere with proteasome-dependent ubiquitination to suppress plant immunity. It would be interesting to establish if this interaction is specific to GpRbp-1 or if StUPL3 is also targeted by other members of the SPRYSEC family. Alternatively, GpRbp-1 may interact with ubiquitin ligases from the plant, such as StUPL3, to activate, modify or utilize other effectors present in the saliva of cyst nematodes, such as GrUBCEP12.

Potato plants lacking StUPL3 might demonstrate if StUPL3 functions as a virulence target of *G. pallida* in potato roots. However, despite several attempts we have not been able to generate a consistent knock-down of StUPL3 expression in roots using virus-induced gene silencing in potato and tomato roots (data not shown). Hence, to better understand the relevance of UPL3 for nematode parasitism, we focused on the role of the *Arabidopsis* UPL3 homologue during infection by cyst nematodes. Previously, AtUPL3 was shown to be required for the development of trichomes by acting as an inhibitor of endoreplication (Downes *et al.*, 2003). Moreover, endoreplication is thought to enable the expansion of nematode-induced syncytia (de Almeida Engler *et al.*, 2012). Given this inhibitory role of AtUPL3, we first hypothesized that this ubiquitin ligase might be recruited by cyst nematodes to regulate the endocycle in syncytia. We reasoned that if AtUPL3 indeed functions as a negative regulator of endoreplication in nematode-induced syncytia, we should find larger syncytia in nematode-infected roots of the *upl3-5* mutant. However, the syncytia established by *H. schachtii* in *upl3-5* mutant plants were slightly smaller than in wild-type *Arabidopsis*. Based on the size of syncytia alone we found no indication that AtUPL3 regulates ploidy levels of syncytial cells. Further direct analysis of the DNA content in syncytial nuclei in the *upl3-5* mutant might provide more conclusive evidence for a role of UPL3 in the regulation of the endocycle in nematode-induced syncytia.

At the transcriptomic level, the subset of differentially expressed genes in nematode-infected roots of *upl3-5* was enriched for genes related to cell division (Fig. 5 and Table S2). *Arabidopsis* homologues of cell cycle control genes *CDC6* and *CDC48* were significantly down-regulated in nematode-infected *upl3-5* as compared to the wild-type (Table S1). Nevertheless, the specific homologues of *CDC6* and *CDC48* significantly regulated in our data are not previously described to have a role in the control of endoreplication or mitosis (Table S1) (Castellano *et al.*, 2001; Copeland *et al.*, 2016; Masuda *et al.*, 2004). Other biological categories found to be enriched in genes differentially regulated in nematode-infected *upl3-5* plants do not indicate further connections to the regulation of the cell cycle or the endoreplication cycle. Altogether, our findings suggest that AtUPL3 does not function as an endocycle regulator during nematode infection in the roots of *Arabidopsis*.

Our data show that although *AtUPL3* may not have a significant effect on the establishment of nematode infection in *Arabidopsis*, female growth and syncytium size, it has a major impact on the transcriptome in nematode-infected roots of

Arabidopsis. Interestingly, a parallel can be drawn with the findings of Furniss *et al.* (2018) where there is a disparity between the relatively small effect of UPL3 on the development of disease symptoms induced by *P. syringae* pv. *maculicola* and the major impact on UPL3-dependent transcriptomic modulation by the exogenous application of SA to *Arabidopsis* plants. In both sets of data there is a minor effect of UPL3 in disease resistance, but a large UPL3-mediated transcriptomic response on the application of an exogenous factor (i.e. SA and nematodes).

Moreover, the set of genes under transcriptional regulation by the combination of UPL3 and nematode infection pointed to stress responses and transcription factor activity. Several genes classified in the gene ontology categories of response to both abiotic and biotic stress and transcription factor activity were differentially regulated in *upl3-5* mutant plants in the presence of cyst nematode infections (Fig. 5; Table 1), including some of the top up-/down-regulated genes. Therefore, UPL3 is likely involved more downstream of syncytium initiation and expansion in host cells as a magnifier of stress responses, in the early stages of infection, which makes host plants more resistant to feeding nematodes. SA is modulated in the early stages of infection with cyst nematodes (Kammerhofer *et al*., 2015), and it is a negative regulator of cyst nematode susceptibility (Kammerhofer *et al*., 2015; Wubben *et al*., 2008; Youssef *et al*., 2013). Given the role of UPL3 as a magnifier of stress responses to SA, we would expect to find an increase in the number of nematodes infecting the roots of *upl3 Arabidopsis*. Therefore, the small decrease in total nematodes infecting the *upl3-5* suggests the existence of mechanisms independent of UPL3, which regulate the cellular components responsible for the SA-mediated inhibition of nematode susceptibility.

Notably, transcription factor MYB121, which is one of the most up-regulated genes in *upl3-5*, has been found to be a high-connectivity regulator of stress response networks mediated by abscisic acid (ABA) in *Arabidopsis* (Carrera *et al*., 2009; Nejat and Mantri, 2017) (Table 1). Also, transcription factor WRKY59, which is one of the most down-regulated genes in *upl3-5* plants, is found to be a transcriptional target of NPR1 during the establishment of SA-mediated systemic acquired resistance (Wang *et al*., 2006) (Table 1). This finding is reminiscent of previous reports where nuclear transcription factors were identified as targets of E3 ligases for regulation of plant physiology and immunity (Serrano *et al*., 2018). We found StUPL3 to be specifically located in the nucleus with a granular pattern that resembles the one reported in *Arabidopsis* for RING-type E3 ligase MIEL1 (Fig. 3) (Marino *et al*., 2013). MIEL1 promotes the proteasomal degradation of transcription factor MYB96 in the absence of ABA (Lee and Seo, 2016). The degradation of MYB96 attenuates ABA-mediated responses to abiotic stress like drought (Seo *et al*., 2009). Additionally, transcription factors from different families have been shown to be involved in plant–nematode interactions (Grunewald *et al*., 2008; Samira *et al*., 2018; Warmerdam *et al*., 2019). For example, WRKY23 from *Arabidopsis* is strongly up-regulated in the early stages of infection by root-knot and cyst nematodes (Grunewald *et al*., 2008). WKRY23 is proposed to be targeted by effectors of *H. schachtii* for establishment of successful feeding sites (Grunewald *et al*., 2008). We therefore hypothesize that UPL3 regulates gene expression at the onset of nematode parasitism through ubiquitination of transcription factors in the nucleus. Furthermore, it is possible that expression of MYB121 and/or WRKY59 is regulated by transcription factors that are in turn targeted for ubiquitination by UPL3, thereby regulating the stress responses of the plant. In turn, the role of UPL3 as regulator of these transcription factors could be stimulated or inhibited by nematodes by means of effectors such as GpRbp-1, to promote susceptibility. An alternative explanation could be that GpRbp-1 requires host factors like UPL3 in order to function properly in the plant cell. Additionally, in order to elucidate the role of the interaction of GpRbp-1 and UPL3, it remains to be seen if GpRbp-1 orthologues are present in *H. schachtii* with similar functional roles to GpRbp-1.

In conclusion, our results suggest that nematode effector GpRbp-1 may manipulate the ubiquitin-proteasome machinery of the host to modulate plant immune responses. On SA treatment, UPL3 has a large impact on total cellular polyubiquitination, suggesting that it may function as a E4 ubiquitin ligase by 'promiscuous' extension of polyubiquitination with low substrate specificity (Furniss *et al*., 2018). Further characterization of the substrate(s) for ubiquitination by UPL3, their subcellular localization and their roles in plant–nematode interactions will lead to additional knowledge on how sedentary nematodes manipulate the (nuclear) ubiquitination machinery of the host to promote susceptibility.

EXPERIMENTAL PROCEDURES

Yeast two-hybrid: library screen

A prey library was generated by Dual Systems Biotech (Switzerland) from ground roots of potato SH infected with juveniles of *G. pallida* population Pa3-Rookmaker. Poly (A) tailing, total RNA isolation, cDNA library construction and yeast two-hybrid screening were performed by Dual Systems Biotech. Further experimental details are provided in Supplemental Text S1.

Yeast two-hybrid: one–one screen

For the reciprocal swap one-to-one yeast two-hybrid the bait GpRbp-1 and prey StUPL3frag8 were exchanged to the prey and bait vectors of the pGAD system (Dual Systems Biotech), respectively. Vectors were co-transformed to PJ69-4a cells, which were then plated onto SD agar base medium without essential amino acids (LEU, TRP, HIS) (TDO). Further experimental details are provided in Supplemental Text S1.

Cloning

For co-IP, the interacting fragment StUPL3frag8 and GpRpb-1 version 1 from virulent population Rookmaker (Rook1) were fused to the respective epitope tags and transferred by restriction enzyme cloning to the pBINPLUS binary vector (van Engelen *et al.*, 1995). For microscopy studies, the full-length gene of StUPL3 was obtained by synthetic gene synthesis (GeneArt) (Thermo Fisher Scientific, Waltham, MA, USA) and cloned to appropriate pGWB vectors (Nakagawa *et al.*, 2007) by Gateway cloning. The mCherry GpRbp-1 construct was generated by restriction enzyme cloning in pBINPLUS (van Engelen *et al.*, 1995). BiFC constructs were generated by Gateway cloning to the pDEST-SCYCE(R)^{GW} and pDEST-SCYNE(R)^{GW} vectors (Gehl *et al.*, 2009). Further experimental details are provided in Supplemental Text S1.

Expression and detection of recombinant proteins

All proteins were co-expressed by *Agrobacterium*-mediated transient transformation of *N. benthamina* leaves. All co-expressions were done together with the silencing suppressor P19, with a final concentration of $OD_{600} = 0.5$. Total protein extracts were prepared by grinding leaf material in protein extraction buffer. For co-IP, pull-downs were performed using MACS anti-c-MYC microbeads (Miltenyi, Bergisch Gladbach, Germany). Proteins were separated by SDS-PAGE on NuPage 12% Bis-Tris gels (Invitrogen, Carlsbad, CA, USA) and blotted to 0.45 μm polyvinylidene difluoride membrane (Thermo Fisher Scientific). Immunodetection was performed with corresponding horseradish peroxidase-conjugated antibodies. Confocal microscopy was performed on *N. benthamiana* epidermal cells using an LSM 510 confocal microscope (Carl-Zeiss, Oberkochen, Germany) with a ×40, 1.2 numerical aperture water-corrected objective. Further details are provided in Supplemental Text S1.

Plant material and nematode infection

Seeds of the homozygous transgenic T-DNA insertion mutant of UPL3 (AT4G38600, line SALK_116326; *upl3-5*) and Col-0 N60000 ecotype were obtained from the SALK homozygote T-DNA collection (Alonso *et al.*, 2003). For nematode infection, seeds were vapour sterilized, sown in Knop's modified medium (Sijmons *et al.*, 1991) and grown at 25 °C under a 16 h light/8 h dark cycle. Ten-day-old seedlings were inoculated with 60–70 surface-sterilized *H. schachtii* infective juveniles. After 2 weeks of infection, the number of nematodes present in the roots of *Arabidopsis* plants was counted visually and the sizes of females and syncytia were determined as described previously (Siddique *et al.*, 2014). Statistical differences were estimated by a fixed-effect model ($\alpha = 0.05$) using the weighted-inverse variants to combine data from four biological replicates. Further details are provided in Supplemental Text S1.

Microarray analysis

Total RNA was extracted from root tissue of non-infected *H. schachtii* or mock-infected seedlings as mentioned previously. Four biological replicates of *c.* 18 plants/sample per condition were generated. cDNA and cRNA were prepared using the Two-Colour Microarray-Based Gene Expression Analysis, Low Input Quick Amp Labelling kit (Agilent Technologies, Santa Clara, CA, USA) according to the manufacturer's instructions. The Arabidopsis V4 Gene Expression Microarray (4 × 44K, Agilent Technologies) probes were compared against the TAIR11 genome of *A. thaliana* (Berardini *et al.*, 2015, Lamesch *et al.*, 2012) using the BLASTN function of the command line BLAST tool (version 2.6.0+, win64), using the default settings. The top-hit was used as probe annotation and probes with multiple hits were censored (Camacho *et al.*, 2009). After hybridization, microarrays were scanned using an Agilent high-resolution C scanner. The scans were extracted using FEATURE EXTRACT (v. 10.7.1.1) and data was normalized in R (v. 3.4.2; R Team, 2014) using the Bioconductor Limma package (Ritchie *et al.*, 2015). Variation attributable to the different conditions was assayed using principal component analysis and differences between genotypes within each condition were tested using a linear model $E_{i,j} = G_j + e$. The obtained significances were corrected for multiple testing using the Benjamini–Hochberg method (Benjamini and Hochberg, 1995) and differentially expressed genes per condition were assessed with a threshold of $-\log_{10}(P) > 4$. To ascertain the biological functions affected, we took a stricter threshold, namely $-\log_{10}(P) > 6$. Enrichments were calculated using a hypergeometric test, as provided in R (phyper). Further details on data preparation and analysis are provided in Supplemental Text S1. The data were submitted to ArrayExpress, code E-MTAB-7968.

ACKNOWLEDGEMENTS

This work was financially supported by the Netherlands Organization for Scientific Research (NWO-ENW) grant 828.11.002 and TTI Green Genetics grant 4CC058RP. The authors would like to thank the Wageningen Light Microscopy Facility and Wageningen Microspectroscopy Research Facility for access to equipment and technical support, Unifarm of Wageningen University and Research for support with plant material and Richard Kormelink for kindly providing pDONOR(207):NSs construct. We are also grateful for technical assistance from Casper van Schaik, Wouter van Bakel, Jorrit Lind and Branimir Velinov, and for statistical advice on methods to combine replicates from Alvaro Muñoz. The authors declare no conflict of interest.

DATA AVAILABILITY STATEMENT

The microarray data that support the findings of this study are openly available in ArrayExpress at https://www.ebi.ac.uk/arrayexpress/, reference number E-MTAB-7968.

REFERENCES

Abramovitch, R.B., Janjusevic, R., Stebbins, C.E. and Martin, G.B. (2006) Type III effector AvrPtoB requires intrinsic E3 ubiquitin ligase activity to suppress plant cell death and immunity. *Proc. Natl. Acad. Sci. USA*, **103**, 2851–2856.

Ali, S., Magne, M., Chen, S., Obradovic, N., Jamshaid, L., Wang, X. and Bélair, G. (2015) Analysis of *Globodera rostochiensis* effectors reveals conserved functions of SPRYSEC proteins in suppressing and eliciting plant immune responses. *Front. Plant Sci.* **6**, 623.

de Almeida Engler, J., Kyndt, T., Vieira, P., Cappelle, E.V., Boudolf, V., Sanchez, V., Escobar, C., De Veylder, L., Engler, G., Abad, P. and Gheysen, G. (2012) *CCS52* and *DEL1* genes are key components of the endocycle in nematode-induced feeding sites. *Plant J.* **72**, 185–198.

Alonso, J.M., Stepanova, A.N., Leisse, T.J., Kim, C.J., Chen, H., Shinn, P., Stevenson, D.K., Zimmerman, J., Barajas, P., Cheuk, R. and Gadrinab, C. (2003) Genome-wide insertional mutagenesis of *Arabidopsis thaliana*. *Science*, **301**, 653–657.

Anwer, M.A., Anjam, M.S., Shah, S.J., Hasan, M.S., Naz, A.A., Grundler, F.M.W. and Siddique, S. (2018) Genome-wide association study uncovers a novel QTL allele of AtS40-3 that affects the sex ratio of cyst nematodes in Arabidopsis. *J. Exp. Bot.* **69**, 1805–1814.

Banfield, M.J. (2015) Perturbation of host ubiquitin systems by plant pathogen/pest effector proteins. *Cell. Microbiol.* **17**, 18–25.

Benjamini, Y. and Hochberg, Y. (1995) Controlling the false discovery rate: a practical and powerful approach to multiple testing. *J. Royal Stat. Soc. Series B (Method).* **57**, 289–300.

Bent, A.F. and Mackey, D. (2007) Elicitors, effectors, and R genes: the new paradigm and a lifetime supply of questions. *Annu. Rev. Phytopathol.* **45**, 399–436.

Berardini, T.Z., Reiser, L., Li, D., Mezheritsky, Y., Muller, R., Strait, E. and Huala, E. (2015) The Arabidopsis information resource: making and mining the "gold standard" annotated reference plant genome. *Genesis*, **53**, 474–485.

Blanchard, A., Esquibet, M., Fouville, D. and Grenier, E. (2005) Ranbpm homologue genes characterised in the cyst nematodes *Globodera pallida* and *Globodera 'mexicana'*. *Physiol. Mol. Plant Pathol.* **67**, 15–22.

Bos, J.I.B., Armstrong, M.R., Gilroy, E.M., Boevink, P.C., Hein, I., Taylor, R.M., Zhendong, T., Engelhardt, S., Vetukuri, R.R., Harrower, B. and Dixelius, C. (2010) *Phytophthora infestans* effector AVR3a is essential for virulence and manipulates plant immunity by stabilizing host E3 ligase CMPG1. *Proc. Natl. Acad. Sci. USA,* **107**, 9909–9914.

Camacho, C., Coulouris, G., Avagyan, V., Ma, N., Papadopoulos, J., Bealer, K. and Madden, T.L. (2009) BLAST+: architecture and applications. *BMC Bioinformatics*, **10**, 421.

Carpentier, J., Esquibet, M., Fouville, D., Manzanares-Dauleux, M.J., Kerlan, M.-C. and Grenier, E. (2012) The evolution of the *Gp-Rbp-1* gene in *Globodera pallida* includes multiple selective replacements. *Mol. Plant Pathol.* **13**, 546–555.

Carrera, J., Rodrigo, G., Jaramillo, A. and Elena, S.F. (2009) Reverse-engineering the *Arabidopsis thaliana* transcriptional network under changing environmental conditions. *Genome Biol.* **10**, R96.

Castellano, M.M., del Pozo, J.C., Ramirez-Parra, E., Brown, S. and Gutierrez, C. (2001) Expression and stability of Arabidopsis CDC6 are associated with endoreplication. *Plant Cell*, **13**, 2671–2686.

Chou, K.-C. and Shen, H.-B. (2007) Large-scale plant protein subcellular location prediction. *J. Cell. Biochem.* **100**, 665–678.

Chou, K.-C. and Shen, H.-B. (2008) Cell-PLoc: a package of Web servers for predicting subcellular localization of proteins in various organisms. *Nat. Protoc.* **3**, 153.

Chou, K.-C. and Shen, H.-B. (2010) Plant-mPLoc: a top-down strategy to augment the power for predicting plant protein subcellular localization. *PLoS ONE*, **5**, e11335.

Chronis, D., Chen, S., Lu, S., Hewezi, T., Carpenter, S.C.D., Loria, R., Baum, T.J. and Wang, X. (2013) A ubiquitin carboxyl extension protein secreted from a plant-parasitic nematode *Globodera rostochiensis* is cleaved *in planta* to promote plant parasitism. *Plant J.* **74**, 185–196.

Copeland, C., Woloshen, V., Huang, Y. and Li, X. (2016) AtCDC48A is involved in the turnover of an NLR immune receptor. *Plant J.* **88**, 294–305.

Craig, A., Ewan, R., Mesmar, J., Gudipati, V. and Sadanandom, A. (2009) E3 ubiquitin ligases and plant innate immunity. *J. Exp. Bot.* **60**, 1123–1132.

Delauré, S.L., Van Hemelrijck, W., De Bolle, M.F.C., Cammue, B.P.A. and De Coninck, B.M.A. (2008) Building up plant defenses by breaking down proteins. *Plant Sci.* **174**, 375–385.

Diaz-Granados, A., Petrescu, A.-J., Goverse, A. and Smant, G. (2016) SPRYSEC effectors: a versatile protein-binding platform to disrupt plant innate immunity. *Front. Plant Sci.* **7**, 1575.

Downes, B.P., Stupar, R.M., Gingerich, D.J. and Vierstra, R.D. (2003) The HECT ubiquitin-protein ligase (UPL) family in Arabidopsis: UPL3 has a specific role in trichome development. *Plant J.* **35**, 729–742.

van Engelen, F.A., Molthoff, J.W., Conner, A.J., Nap, J.P., Pereira, A. and Stiekema, W.J. (1995) pBINPLUS: an improved plant transformation vector based on pBIN19. *Transgenic Res.* **4**, 288–290.

Furniss, J.J., Grey, H., Wang, Z., Nomoto, M., Jackson, L., Tada, Y. and Spoel, S.H. (2018) Proteasome-associated HECT-type ubiquitin ligase activity is required for plant immunity. *PLoS Pathog.* **14**, e1007447.

Gehl, C., Waadt, R., Kudla, J., Mendel, R.-R. and Hänsch, R. (2009) New GATEWAY vectors for high throughput analyses of protein–protein interactions by bimolecular fluorescence complementation. *Mol. Plant*, **2**, 1051–1058.

Gheysen, G. and Mitchum, M.G. (2011) How nematodes manipulate plant development pathways for infection. *Curr. Opin. Plant Biol.* **14**, 415–421.

Grunewald, W., Karimi, M., Wieczorek, K., Van de Cappelle, E., Wischnitzki, E., Grundler, F., Inzé, D., Beeckman, T. and Gheysen, G. (2008) A role for AtWRKY23 in feeding site establishment of plant-parasitic nematodes. *Plant Physiol.* **148**, 358–368.

Hewezi, T. (2015) Cellular signaling pathways and post-translational modifications mediated by nematode effector proteins. *Plant Physiol.* **169**, 1018–1026.

Hewezi, T., Piya, S., Qi, M., Balasubramaniam, M., Rice, J.H. and Baum, T.J. (2016) Arabidopsis miR827 mediates post-transcriptional gene silencing of its ubiquitin E3 ligase target gene in the syncytium of the cyst nematode *Heterodera schachtii* to enhance susceptibility. *Plant J.* **88**, 179–192.

Hirsch, C.D., Hamilton, J.P., Childs, K.L., Cepela, J., Crisovan, E., Vaillancourt, B., Hirsch, C.N., Habermann, M., Neal, B. and Buell, C.R. (2014) Spud DB: a resource for mining sequences, genotypes, and phenotypes to accelerate potato breeding. *Plant Genome*, 7. doi: 10.3835/plantgenome2013.12.0042.

Hofmann, J. and Grundler, F. (2007) Identification of reference genes for qRT-PCR studies of gene expression in giant cells and syncytia induced in *Arabidopsis thaliana* by *Meloidogyne incognita* and *Heterodera schachtii*. *Nematology*, **9**, 317–323.

Jones, J.T., Kumar, A., Pylypenko, L.A., Thirugnanasambandam, A., Castelli, L., Chapman, S., Cock, P.J., Grenier, E., Lilley, C.J., Phillips, M.S. and Blok, V.C. (2009) Identification and functional characterization of effectors in expressed sequence tags from various life cycle stages of the potato cyst nematode *Globodera pallida*. *Mol. Plant Pathol.* **10**, 815–828.

Juvale, P.S. and Baum, T.J. (2018) "Cyst-ained" research into *Heterodera* parasitism. *PLoS Pathog.* **14**, e1006791.

Kammerhofer, N., Radakovic, Z., Regis, J.M., Dobrev, P., Vankova, R., Grundler, F.M., Siddique, S., Hofmann, J. and Wieczorek, K. (2015) Role of stress-related hormones in plant defence during early infection of the cyst nematode *Heterodera schachtii* in Arabidopsis. *New Phytol.* **207**, 778–789.

Klepikova, A.V., Kasianov, A.S., Gerasimov, E.S., Logacheva, M.D. and Penin, A.A. (2016) A high resolution map of the *Arabidopsis thaliana* developmental transcriptome based on RNA-seq profiling. *Plant J.* **88**, 1058–1070.

Kosugi, S., Hasebe, M., Entani, T., Takayama, S., Tomita, M. and Yanagawa, H. (2008) Design of peptide inhibitors for the importin alpha/beta nuclear import pathway by activity-based profiling. *Chem. Biol.* **15**, 940–949.

Kosugi, S., Hasebe, M., Matsumura, N., Takashima, H., Miyamoto-Sato, E., Tomita, M. and Yanagawa, H. (2009a) Six classes of nuclear localization signals specific to different binding grooves of importin α. *J. Biol. Chem.* **284**, 478–485.

Kosugi, S., Hasebe, M., Tomita, M. and Yanagawa, H. (2009b) Systematic identification of cell cycle-dependent yeast nucleocytoplasmic shuttling proteins by prediction of composite motifs. *Proc. Natl. Acad. Sci. USA*, **106**, 10171–10176.

Krishnakumar, V., Hanlon, M.R., Contrino, S., Ferlanti, E.S., Karamycheva, S., Kim, M., Rosen, B.D., Cheng, C.-Y., Moreira, W., Mock, S.A., Stubbs, J., Sullivan, J.M., Krampis, K., Miller, J.R., Micklem, G., Vaughn, M. and Town, C.D. (2015) Araport: the Arabidopsis information portal. *Nucleic Acids Res.* **43**, D1003–D1009.

Kud, J., Wang, W., Gross, R., Fan, Y., Huang, L., Yuan, Y., Gray, A., Duarte, A., Kuhl, J.C., Caplan, A., Goverse, A., Liu, Y., Dandurand, L.-M. and Xiao, F. (2019) The potato cyst nematode effector RHA1B is a ubiquitin ligase and uses two distinct mechanisms to suppress plant immune signaling. *PLoS Pathog.* **15**, e1007720.

Lamesch, P., Berardini, T.Z., Li, D., Swarbreck, D., Wilks, C., Sasidharan, R., Muller, R., Dreher, K., Alexander, D.L., Garcia-Hernandez, M., Karthikeyan, A.S., Lee, C.H., Nelson, W.D., Ploetz, L., Singh, S., Wensel, A. and Huala, E. (2012) The Arabidopsis Information Resource (TAIR): improved gene annotation and new tools. *Nucleic Acids Res.* **40**, D1202–D1210.

Lee, H.G. and Seo, P.J. (2016) The Arabidopsis MIEL1 E3 ligase negatively regulates ABA signalling by promoting protein turnover of MYB96. *Nat. Commun.* **7**, 12525.

Marchler-Bauer, A. and Bryant, S.H. (2004) CD-Search: protein domain annotations on the fly. *Nucleic Acids Res.* **32**, W327–W331.

Marchler-Bauer, A., Bo, Y., Han, L., He, J., Lanczycki, C.J., Lu, S., Chitsaz, F., Derbyshire, M.K., Geer, R.C., Gonzales, N.R., Gwadz, M., Hurwitz, D.I., Lu, F., Marchler, G.H., Song, J.S., Thanki, N., Wang, Z., Yamashita, R.A., Zhang, D., Zheng, C., Geer, L.Y. and Bryant, S.H. (2017) CDD/SPARCLE: functional classification of proteins via subfamily domain architectures. *Nucleic Acids Res.* **45**, D200–D203.

Marino, D., Froidure, S., Canonne, J., Ben Khaled, S., Khafif, M., Pouzet, C., Jauneau, A., Roby, D. and Rivas, S. (2013) Arabidopsis ubiquitin ligase MIEL1 mediates degradation of the transcription factor MYB30 weakening plant defence. *Nat. Commun.* **4**, 1476.

Masuda, H.P., Ramos, G.B.A., de Almeida-Engler, J., Cabral, L.M., Coqueiro, V.M., Macrini, C.M.T., Ferreira, P.C.G. and Hemerly, A.S. (2004) Genome based identification and analysis of the pre-replicative complex of *Arabidopsis thaliana*. *FEBS Lett.* **574**, 192–202.

Mazzucotelli, E., Belloni, S., Marone, D., De Leonardis, A.M., Guerra, D., Di Fonzo, N., Cattivelli, L. and Mastrangelo, A.M. (2006) The E3 ubiquitin ligase gene family in plants: regulation by degradation. *Curr. Genomics*, **7**, 509–522.

Mei, Y., Wright, K.M., Haegeman, A., Bauters, L., Diaz-Granados, A., Goverse, A., Gheysen, G., Jones, J.T. and Mantelin, S. (2018) The *Globodera pallida* SPRYSEC effector GpSPRY-414-2 that suppresses plant defenses targets a regulatory component of the dynamic microtubule network. *Front. Plant Sci.* **9**, 1019.

Miricescu, A., Goslin, K. and Graciet, E. (2018) Ubiquitylation in plants: signaling hub for the integration of environmental signals. *J. Exp. Bot.* **69**, 4511–4527.

Mitchum, M.G., Hussey, R.S., Baum, T.J., Wang, X., Elling, A.A., Wubben, M. and Davis, E.L. (2013) Nematode effector proteins: an emerging paradigm of parasitism. *New Phytol.* **199**, 879–894.

Nakagawa, T., Kurose, T., Hino, T., Tanaka, K., Kawamukai, M., Niwa, Y., Toyooka, K., Matsuoka, K., Jinbo, T. and Kimura, T. (2007) Development of series of gateway binary vectors, pGWBs, for realizing efficient construction of fusion genes for plant transformation. *J. Biosci. Bioeng.* **104**, 34–41.

Nakamura, Y., Gojobori, T. and Ikemura, T. (2000) Codon usage tabulated from international DNA sequence databases: status for the year 2000. *Nucleic Acids Res.* **28**, 292.

Nejat, N. and Mantri, N. (2017) Plant immune system: crosstalk between responses to biotic and abiotic stresses the missing link in understanding plant defence. *Curr. Issues Mol. Biol.* **23**, 1–16.

Nicol, J.M., Turner, S.J., Coyne, D.L., Nijs, L.d., Hockland, S. and Maafi, Z.T. (2011) Current nematode threats to world agriculture. In: Genomics and Molecular Genetics of Plant-Nematode Interactions. (Jones, J., Gheysen, G. and Fenoll, C., eds), pp. 21–43. Dordrecht: Springer, Netherlands.

Patra, B., Pattanaik, S. and Yuan, L. (2013) Ubiquitin protein ligase 3 mediates the proteasomal degradation of GLABROUS 3 and ENHANCER OF GLABROUS 3, regulators of trichome development and flavonoid biosynthesis in Arabidopsis. *Plant J.* **74**, 435–447.

Pieterse, C.M.J., Does, D.V.d., Zamioudis, C., Leon-Reyes, A. and Wees, S.C.M.V. (2012) Hormonal modulation of plant immunity. *Annu. Rev. Cell. Dev. Biol.* **28**, 489–521.

Quentin, M., Abad, P. and Favery, B. (2013) Plant parasitic nematode effectors target host defense and nuclear functions to establish feeding cells. *Front. Plant Sci.* **4**, 53.

Rehman, S., Postma, W., Tytgat, T., Prins, P., Qin, L., Overmars, H., Vossen, J., Spiridon, L.N., Petrescu, A.J., Goverse, A. and Bakker, J. (2009) A secreted SPRY domain-containing protein (SPRYSEC) from the plant-parasitic nematode *Globodera rostochiensis* interacts with a CC-NB-LRR protein from a susceptible tomato. *Mol. Plant–Microbe Interact.* **22**, 330–340.

Ritchie, M.E., Phipson, B., Wu, D., Hu, Y., Law, C.W., Shi, W. and Smyth, G.K. (2015) limma powers differential expression analyses for RNA-sequencing and microarray studies. *Nucleic Acids Res.* **43**, e47.

Sacco, M.A., Koropacka, K., Grenier, E., Jaubert, M.J., Blanchard, A., Goverse, A., Smant, G. and Moffett, P. (2009) The cyst nematode SPRYSEC protein RBP-1 elicits Gpa2- and RanGAP2-dependent plant cell death. *PLoS Pathog.* **5**, e1000564.

Sadanandom, A., Bailey, M., Ewan, R., Lee, J. and Nelis, S. (2012) The ubiquitin–proteasome system: central modifier of plant signalling. *New Phytol.* **196**, 13–28.

Samira, R., Li, B., Kliebenstein, D., Li, C., Davis, E., Gillikin, J.W. and Long, T.A. (2018) The bHLH transcription factor ILR3 modulates multiple stress responses in Arabidopsis. *Plant Mol. Biol.* **97**, 297–309.

Schmid, M., Davison, T.S., Henz, S.R., Pape, U.J., Demar, M., Vingron, M., Schölkopf, B., Weigel, D. and Lohmann, J.U. (2005) A gene expression map of *Arabidopsis thaliana* development. *Nat. Genet.* **37**, 501–506.

Seo, P.J., Xiang, F., Qiao, M., Park, J.-Y., Lee, Y.N., Kim, S.-G., Lee, Y.H., Park, W.J. and Park, C.M. (2009) The MYB96 transcription factor mediates abscisic acid signaling during drought stress response in Arabidopsis. *Plant Physiol.* **151**, 275–289.

Serrano, I., Campos, L. and Rivas, S. (2018) Roles of E3 ubiquitin-ligases in nuclear protein homeostasis during plant stress responses. *Front Plant Sci.* **9**, 139.

Shen, H.-B. and Chou, K.-C. (2006) Ensemble classifier for protein fold pattern recognition. *Bioinformatics*, **22**, 1717–1722.

Shu, K. and Yang, W. (2017) E3 ubiquitin ligases: ubiquitous actors in plant development and abiotic stress responses. *Plant Cell Physiol.* **58**, 1461–1476.

Siddique, S., Matera, C., Radakovic, Z.S., Shamim Hasan, M., Gutbrod, P., Rozanska, E., Sobczak, M., Torres, M.A. and Grundler, F.M.W. (2014) Parasitic worms stimulate host NADPH oxidases to produce reactive oxygen species that limit plant cell death and promote infection. *Sci. Signal*, **7**, ra33.

Sijmons, P.C., Grundler, F.M.W., Mende, N., Burrows, P.R. and Wyss, U. (1991) *Arabidopsis thaliana* as a new model host for plant-parasitic nematodes. *Plant J.* **1**, 245–254.

Smyth, G.K. and Speed, T. (2003) Normalization of cDNA microarray data. *Methods*, **31**, 265–273.

Sperschneider, J., Catanzariti, A.-M., DeBoer, K., Petre, B., Gardiner, D.M., Singh, K.B., Dodds, P.N. and Taylor, J.M. (2017) LOCALIZER: subcellular localization prediction of both plant and effector proteins in the plant cell. *Sci. Rep.* **7**, 44598.

R Team (2014) R: A Language and Environment for Statistical Computing. Vienna, Austria: R Foundation for Statistical Computing.

Thimm, O., Bläsing, O., Gibon, Y., Nagel, A., Meyer, S., Krüger, P., Selbig, J., Müller, L.A., Rhee, S.Y. and Stitt, M. (2004) mapman: a user-driven tool to display genomics data sets onto diagrams of metabolic pathways and other biological processes. *Plant J.* **37**, 914–939.

Ustun, S., Sheikh, A., Gimenez-Ibanez, S., Jones, A., Ntoukakis, V. and Bornke, F. (2016) The proteasome acts as a hub for plant immunity and is targeted by *Pseudomonas* type III effectors. *Plant Physiol.* **172**, 1941–1958.

Vandesompele, J., De Preter, K., Pattyn, F., Poppe, B., Van Roy, N., De Paepe, A. and Speleman, F. (2002) Accurate normalization of real-time quantitative RT-PCR data by geometric averaging of multiple internal control genes. *Genome Biol.* **3**, research0034.0031.

Vierstra, R.D. (2009) The ubiquitin–26S proteasome system at the nexus of plant biology. *Nat. Rev. Mol. Cell Biol.* **10**, 385.

Waese, J., Fan, J., Pasha, A., Yu, H., Fucile, G., Shi, R., Cumming, M., Kelley, L.A., Sternberg, M.J., Krishnakumar, V., Ferlanti, E., Miller, J., Town, C., Stuerzlinger, W. and Provart, N.J. (2017) ePlant: visualizing and exploring multiple levels of data for hypothesis generation in plant biology. *Plant Cell*, **29**, 1806–1821.

Wang, D., Amornsiripanitch, N. and Dong, X. (2006) A genomic approach to identify regulatory nodes in the transcriptional network of systemic acquired resistance in plants. *PLoS Pathog.* **2**, e123.

Warmerdam, S., Sterken, M.G., Van Schaik, C., Oortwijn, M.E.P., Lozano-Torres, J.L., Bakker, J., Goverse, A. and Smant, G. (2019) Mediator of tolerance to abiotic stress ERF6 regulates susceptibility of Arabidopsis to *Meloidogyne incognita*. *Mol. Plant Pathol.* **20**, 137–152.

Wubben, M.J., Jin, J. and Baum, T.J. (2008) Cyst nematode parasitism of *Arabidopsis thaliana* is inhibited by salicylic acid (SA) and elicits uncoupled SA-independent pathogenesis-related gene expression in roots. *Mol. Plant–Microbe Interact.* **21**, 424–432.

Yachdav, G., Kloppmann, E., Kajan, L., Hecht, M., Goldberg, T., Hamp, T., Hönigschmid, P., Schafferhans, A., Roos, M., Bernhofer, M., Richter, L., Ashkenazy, H., Punta, M., Schlessinger, A., Bromberg, Y., Schneider, R., Vriend, G., Sander, C., Ben-Tal, N. and Rost, B. (2014) PredictProtein – an open resource for online prediction of protein structural and functional features. *Nucleic Acids Res.* **42**, W337–W343.

Youssef, R.M., MacDonald, M.H., Brewer, E.P., Bauchan, G.R., Kim, K.-H. and Matthews, B.F. (2013) Ectopic expression of AtPAD4 broadens resistance of soybean to soybean cyst and root-knot nematodes. *BMC Plant Biol.* **13**, 67.

Zahurak, M., Parmigiani, G., Yu, W., Scharpf, R.B., Berman, D., Schaeffer, E., Shabbeer, S. and Cope, L. (2007) Pre-processing Agilent microarray data. *BMC Bioinformatics*, **8**, 142.

Zhou, B. and Zeng, L. (2017) Conventional and unconventional ubiquitination in plant immunity. *Mol. Plant Pathol.* **18**, 1313–1330.

SUPPORTING INFORMATION

Additional supporting information may be found in the online version of this article at the publisher's web site:

Fig. S1 Characterization of the potato homologue of UPL3. (A) Protein sequence alignment of full-length AtUPL3 and StUPL3. Protein sequences were obtained by translation in frame +1 of the AtUPL3 CDS (AtUPL3; AT4G38600), the predicted StUPL3 promotes polyubiquitination *in planta*. E3 ubiquitin-protein ligase from GenBank (StUPL3 NCBI; XM_015314510), the combination of Spubdb transcripts PGSC0003DMT400031189 and PGSC0003DMT400031190 (StUPL3Comb) (Hirsch *et al.*, 2014) and the yeast interacting fragment (StUPL3frag8). The alignment was made with the CLUSTALW plugin of Geneious (v. 8.1.9) with cost matrix BLOSUM. Identical amino acids are highlighted in dark grey. Predicted NLSs are shown with a yellow box, the Armadillo repeats domain is indicated by a green box, the HECT domain is shown with a blue box and the E2 interaction site is shown with a red bar. (B) StUPL3 promotes polyubiquitination *in planta*. *Agrobacterium tumefaciens* GV2260 harbouring the epitope-tagged ubiquitin (HA-Ub) or StUPL3 (GFP-StUPL3 or HA-StUPL3) as an indicated combination were infiltrated into *Nicotiana benthamiana* leaves at a concentration of OD_{600} = 0.2. *Agrobacterium tumefaciens* containing the empty vector (EV) was used as a control. Forty-eight hours after *Agrobacterium* infiltration, proteins were extracted for western blotting assay using α-HA antibody to determine polyubiquitination, which appears as a smear banding pattern.

Fig. S2 Individual bimolecular fluorescence complementation protein fusions do not emit fluorescence, despite appropriate expression *in planta*. (A) Live imaging of individual N-CFP (pN) or C-CFP (pC) fusions to StUPL3 and GpRbp-1. A CFP transformation is shown for comparison of the confocal microscopy settings. (B) Western blot detection with anti-FLAG (pN constructs) and anti-HA (pC constructs).

Fig. S3 Fluorescent fusions of StUPL3 and GpRbp-1 are expressed by agroinfiltration. Western blot detection of fusions of fluorescent proteins green fluorescent protein with StUPL3 (GFP-UPL3), red fluorescent protein mCherry (mCh-GpRbp-1) or GFP and mCh alone. Western blot was performed with anti-GFP and anti-RFP antibodies.

Fig. S4 AtUPL3 is not regulated during cyst-nematode infection in the roots of *Arabidopsis thaliana*. Expression of AtUPL3 was quantified by Reverse transcriptase polymerase chain reaction (RT-PCR) in *A. thaliana* roots infected with cyst nematode *Heterodera schachtii*. The ratio of AtUPL3 expression was normalized to the geometric average of ubiquitin 5 (Anwer *et al.*, 2018) and ubiquitin carboxyl-terminal hydrolase 22 (Hofmann & Grundler, 2007) using the Vandesompele method (Vandesompele *et al.*, 2002).

Fig. S5 Principal component analysis of gene expression profiles of *upl3-5* and wild-type *Arabidopsis* plants before infection and 7 days after (mock) infection. The first principal component (PCO 1) captures 46.1% of the variation and separates the age of the *Arabidopsis* seedlings. The second principal component (PCO 2) captures 21.9% of variation and separates infected from uninfected samples.

Fig. S6 The top two most down-/up-regulated genes by size of the effect in nematode-infected *upl3-5 Arabidopsis* show a similar pattern of expression. (A) Developmental expression of a

predicted member of the RmIC-cupin superfamily (AT3G05950) and (C) predicted CAP-superfamily member (AT4G07820) (Schmid *et al.*, 2005, Waese *et al.*, 2017). (B) RNA-Seq based expression of a predicted member of the RmIC-cupin superfamily (AT3G05950) and (D) predicted CAP-superfamily member (AT4G07820) (Waese *et al.*, 2017, Klepikova *et al.*, 2016). (E) Heatmap of expression of a predicted member of the RmIC-cupin superfamily (AT3G05950), a predicted CAP-superfamily member (AT4G07820) and AtUPL3 (At4G38600) across 350+ samples from the ePlant collection (ePlant HeatMap Viewer tool and references therein) (Waese *et al.*, 2017). Colours are drawn according to the local maximums.

Table S1 A list of all the genes significantly regulated in *upl3-5* plants. The treatment column indicates which comparison was made. The significance column gives the significance of the difference as determined by the linear model, the effect column the size of the difference (log_2-units; negative values are less expressed in Col-0, positive values more expressed in Col-0). The significance_FDR column lists the *q* values as determined by Benjamini–Hochberg correction. The columns thereafter list properties of the genes detected by the spots. Spots with no associated gene are either technical spots or have significant BLAST hits with multiple different genes. If this is the case, it is mentioned in the comments. The genes are selected by the $-\log_{10}(P) < 4$ (yellow) or $-\log_{10}(P) < 6$ (red) thresholds.

Table S2 Enrichment analysis of the 131 differentially expressed genes between Col-0 and *upl3-5* on infection with *Heterodera schachtii*. Groups found to be enriched in the genes that are differentially regulated in *upl3-5* during nematode infection. The groups are categorized by the significance of the enrichment (significance FDR). The annotation database, number of genes present per group in the database, the overlap expected by random and the calculated overlap are also shown.

Table S3 List of primers and sequences mentioned in the text.

Text S1 Supporting experimental procedures.